Chapter 2 Simulation of Single Walled Carbon Nano Tubes (SWNT)

2.1 Introduction

Carbon nanotubes were discovered in 1991 by Iijima of NEC Corporation.[1] Since then, efforts in synthesis, characterization, and theoretical investigation have grown exponentially. This is mostly due to their perceived novel mechanical and electronic properties and their tremendous potential for future technological applications. In 1993, the simplest kind of carbon nanotubes, single-walled carbon nanotubes were discovered independently by Iijima's group[2] and an IBM team headed by Bethune.[3] These SWNTs can be regarded as rolled-up graphite sheets in the cylindrical form. Some specific defect-free forms of SWNTs showed remarkable mechanical properties and metalic behavior.[4] These materials present tremendous potential as components for use in nano electronic and nano-mechanical applications, or as structural elements in various devices.

Thess and co-workers[4] later produced crystalline "ropes" of metallic carbon nanotubes with 100 to 500 SWNTs bundled into a two-dimensional triangular lattice. These tightly bundled linear "ropes" are expected to have remarkable mechanical properties, as well as superior electronic and magnetic properties. Various levels of studies were performed on the properties of SWNTs, including use of classical molecular mechanics, molecular dynamcis, and tight binding level quantum mechanical methods.[5−12]

In this chapter, we present a detailed study of the energetics, structures, and

[1]Based on "Energetics, structure, mechanical and vibrational properties of single-walled carbon nano tubes (SWNT)," **G. Gao, T. Cagin, and W.A., Goddard III**, presented on Fifth Foresight Conference on Molecular Nanotechnology

mechanical properties of single-walled carbon nano tubes with different radius and chirality (armchair (n, n), chiral (2n, n), and zigzag (n, 0)). We used an accurate force field, derived through quantum calculation, to represent the interactions between the carbon atoms.[13] These interaction potentials were used earlier in studying structure, mechanical and vibrational properties of graphite, various fullerenes and intercated compounds of fullerenes,[14] and nano tubes.[15] In our studies, we employed classical molecular dynamics and molecular mechanics methods as implemented in MPSim (a massively parallel program for materials simulations) program.[16] Molecular dynamics runs are made to anneal the structures, whereas molecular mechanics, energy and/or enthalpy minimization, are applied at the end of annealing cycle to obtain the final optimized structures. Using the analytical second derivatives of the potential energy, we also calculated the vibrational modes and frequencies of three kinds of nanotube bundles, (10, 10) armchair, (17, 0) zig-zag and (12, 6) chiral. These tubes have comparable cross section diameters, and are among the easiest to make.

2.2 Energetics and the Stability of Circular versus Collapsed Tubes

In order to assess the mechanical stability of various SWNTs, we created three chiral forms ((n, n) armchair, (n, 0) zigzag, and (2n, n) chiral) with various diameters. For each form, we studied two sets of initial structures, perfect circular cross section and elongated or collapsed cross section. For the collapsed structures, the opposit walls in the middle section are within van der Waals attraction distance and the shape of the two ends is close to circular with diameter of D $\sim$ 10.7 (Å) (Fig. 2.2). To mimic long isolated nanotube, we imposed periodic boundary condition in c-direction (tube axis). To eliminate inter tube interactions, we set the cell parameters a and b as 50 times of the circular tube diameter. Energy and structural optimizition were carried out using MPSim. Figure 2.1 is the strain energy per carbon atom

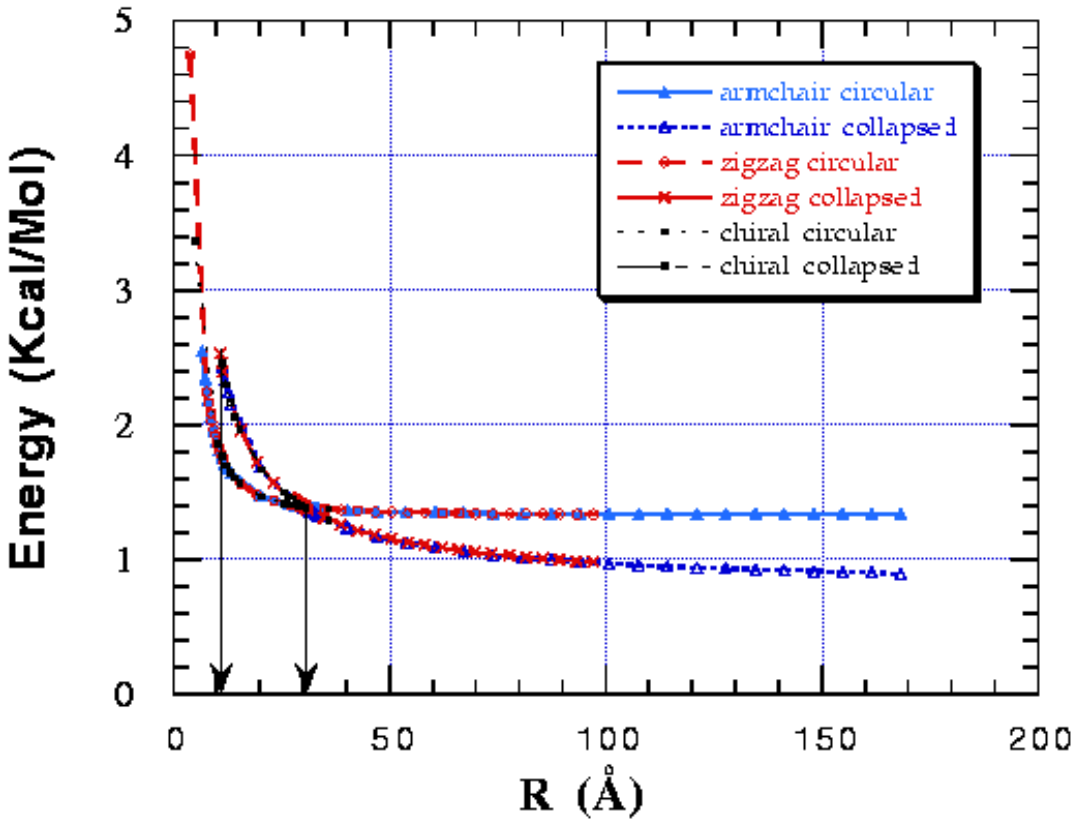

Figure 2.1: Energy per carbon atom (relative to graphite) of stable structures for (n, n), (n, 0), and (2n, n) SWNTs; R is the radius of its circular structure.

versus radius of its circular form. We put the two sets (collapsed versus circular) with three chiral forms (armchair (n, n), chiral (2n, n), and zigzag (n, 0)) on the same plot. For all three forms, there are three regions associated with two transition radii (R_1 and R_2). For tubes with circular radius smaller than R_1, only the circular form is existed, the collapsed initial structure recovered to the circular form during structural optimization. For tubes with circular radius between R_1 and R_2, there are two stable structures with the circular structure more stable. For tubes with circular radius larger than R_2, collapsed form becomes energetically favored while the circular form becomes meta-stable. The structures and radii of the first transition are:

- (n, n) armchair, R_1 is between 10.77 (Å) of (16, 16) and 11.44 (Å) of (17, 17).

Figure 2.2: Starting structures for circular and collapsed tubes

- (2n, n) chiral, R_1 is between 10.28 Å) of (20, 10) and 11.31 (Å) of (22, 11).
- (n, 0) zigzag, R_1 is between 10.49 (Å) of (27, 0) and 10.88 (Å) of (28, 0).

The structures and the radii of the second transition are:

- (n, n) armchair, R_2 is between 29.62 (Å) of (45, 45) and 30.30 (Å) of (46, 46).
- (2n, n) chiral, R_2 is between 29.82 (Å) of (58, 29)) and 30.85 (Å) of (60, 30).
- (n, 0) zigzag, R_2 is between 29.93 (Å) of (77, 0) and 30.32 (Å) of (78, 0).

Looking at the collapsed structures of various radii along tube axis, we found that they all have two circular (or elliptical) ends of diameter D $\sim$ 10.5 (Å) and flat middle section. The inter wall distances in the flat region are close to 3.4 (Å), which is the inter layer distance of adjacent graphite sheets. The ends sections are highly strained compared to the circular form, thus cost energy. In addition to zero strain energy, the flat region is further stablized by inter layer van der Waals attractions. The relative strength of these two opposite forces dictates the two structural transformations. Shown in Fig. 2.3 are optimized structures of armchair (n, n) tubes with collapsed initial structure. The zigzag (n, 0) and chiral (2n, n) tubes are the same.

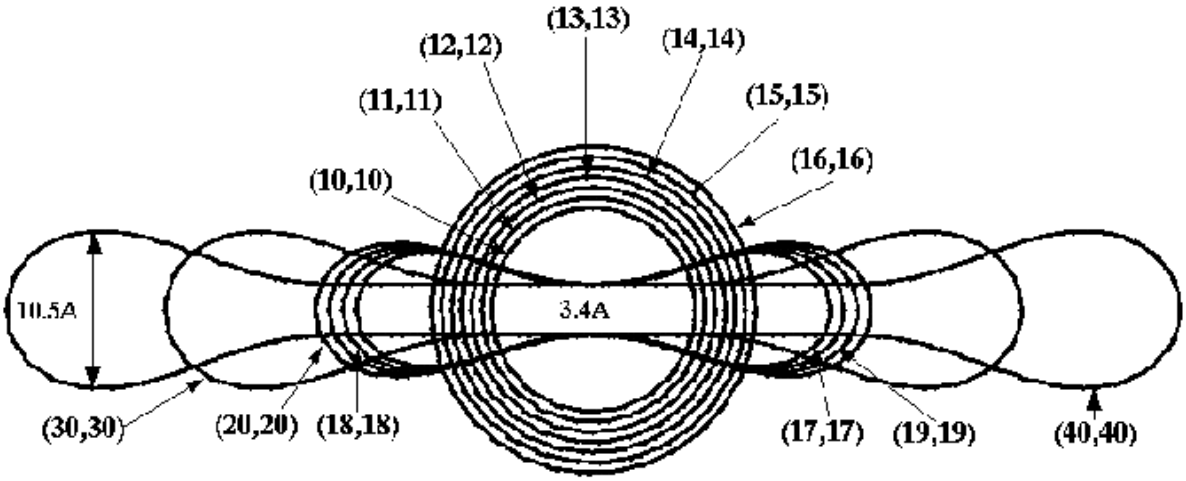

Figure 2.3: Cross section of optimum tube structures (started from collapsed form)

Based on the optimized structures and their energies of the circular form, we can model the basic energetics by approximating the tube as a membrane with a curvature of 1/R and bending modulus[17] of κ. Assuming a as the thickness of tube wall, the elastic energy stored in a slab of width L is given by $\pi\kappa La^2/(12R)$. The per atom energy can be written as

$$E_C = \frac{\pi\kappa La^2}{12RN} + E_\infty \tag{2.1}$$

where N is the number of carbon atoms per slab and E_∞ is energy per carbon atom for tubes with $R \sim \infty$, i.e., flat sheets. Considering ρ as the number of carbon atoms per unit area of tube wall, we have

$$E_C = \kappa\frac{a^2}{24\rho}\frac{1}{R^2} + E_\infty \tag{2.2}$$

Setting a as the spacing between two graphite sheets, 3.335 (Å), $R_o = 1.410$ (Å) as the C-C bond distance, we obtained $\kappa_{(n,n)} = 963.44$ (GPa), $\kappa_{(n,0)} = 911.64$ (GPa), and $\kappa_{(2n,n)} = 935.48$ (GPa). These results are plotted against the theoretical estimates in Fig. 2.4.

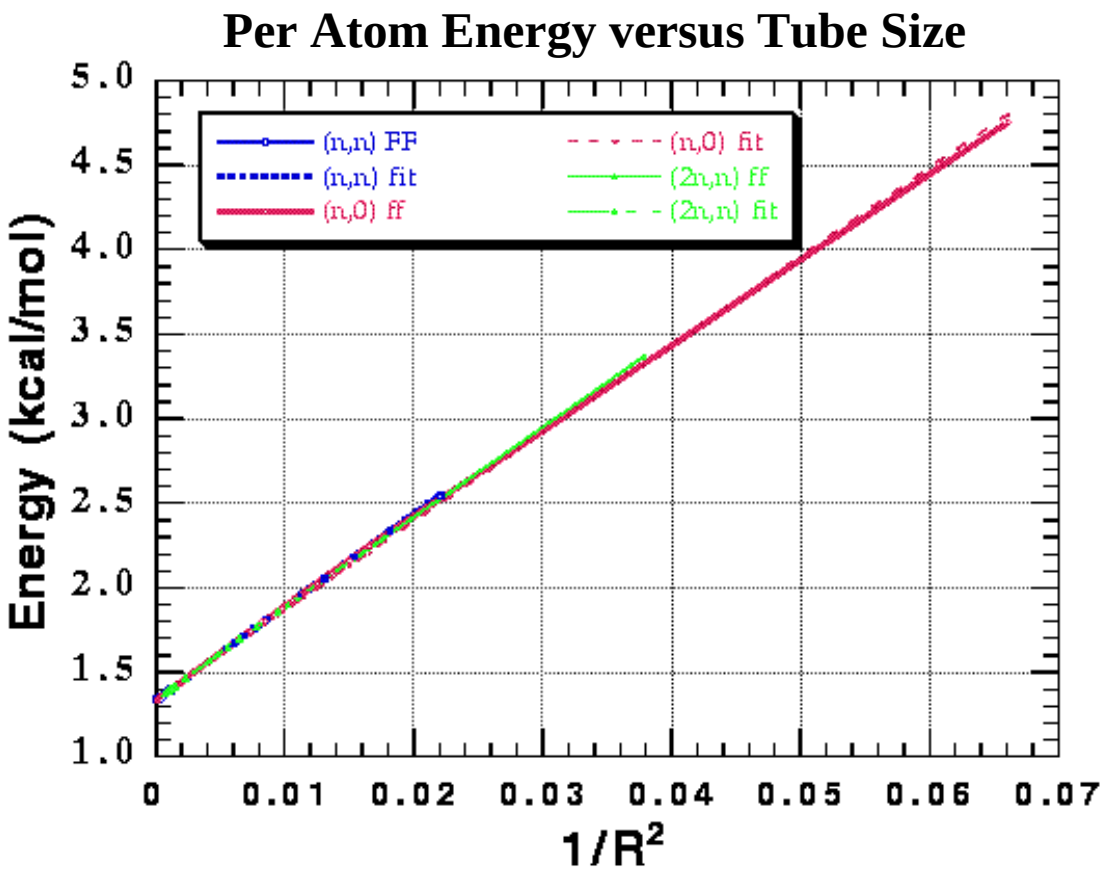

Figure 2.4: Energy per atom versus square of tube curvature

The bending modulus of sheets with different chirality suggest that the transition radius depends on the chirality, with (2n, n) transition radius larger than that of (n, 0) zigzag, but smaller than that of (n, n) armchair. That is what we expected, because the higher the bending modulus, the higher the strain energy. The (n, n) armchair has higher binding energy than that of (2n, n), while the (n, 0) zigzag has lower binding energy than that of (2n, n). However, by examining the collapsed structures closely, we also found different inter layer stacking in the collapsed region. Figure 2.5 is the side views of the two attracting layers for three cases. The inter-layer stacking patterns are different due to different chirality. The inter-layer distances are also differ slightly, with $d_{(n,n)} = 3.38$ (Å), $d_{(2n,n)} = 3.39$ (Å), and $d_{(n,0)} = 3.41$ (Å).

Energetically, inter-layer attraction of armchair is the best with per atom energy of E = 0.7336 (kcal/mol), and stacking of the opposite walls is almost identical to the graphite stacking. The inter-layer attraction in the zigzag form is the worst with per atom energy, E = 0.7439 (kcal/mol), since the carbon atoms on different layers are lined up on top of each other. The attraction energy per atom for the collapsed (2n, n) chiral nanotube is between the two. Overall, the two factors (bending modulus and van der Waals attraction) cancels out for different chirality, so that in terms of transition radius and the cross-over radius, the size of the circular tube (radius) is the dominant factor in deciding the stable forms.

2.3 Structure and Mechanical Properties of Packed SWNT Crystals

Among various conformations, the (10, 10) SWNT is the easiest to make. We studied the mechanical properties of its bulk phase (tube bundles). We also calculated the bulk properties of (17, 0) zigzag and (12, 6) chiral tubes, with cross section radii close to that of (10, 10) tube. Molecular dynamics and molecular mechanics studies led to a triangular packing as the most stable structure for all three forms. The triangular lattice parameter for armchair (10, 10) is $a = 16.78$ (Å) with density of $\rho = 1.33$ (g/cc). For the zigzag (17, 0), they are $a = 16.52$ (Å) and $\rho = 1.34$ (g/cc). For the chiral form (12, 6), they are $a = 15.62$ (Å) and $\rho = 1.40$ (g/cc). More importantly, we determined the Young's modulus along the tube axis for triangular-packed SWNTs using the second derivatives of the potential energy. They are Y = 640.30 (GPa), Y = 648.43 (GPa), and Y = 673.49 (GPa), respectively. Normalized to carbon sheet, these values are within a few percent of the graphite bulk value.

2.4 Vibrational Modes and Frequencies of SWNTs

We calculated the vibrational modes and frequencies of (10, 10) tube crystals. Due to their comparable tube radius with respect to (10, 10) tube, zigzag (17, 0) and chiral (12, 6) tube crystals are also studied. These results can be used to differentiate chiral tubes with comparable diameters. In Table 2.1, B denotes breathing mode as displayed in Fig. 2.6b, S stands for shearing mode as in Fig. 2.6c, and C stands for cyclopes as in Fig. 2.6d. The uniform compression mode is also shown in Fig. 2.6a and occurs at 186 cm^{-1} for (10, 10), which is exactly the same as the experimental frequency[18]. We tabulated the uniform compression mode and highest graphite in-plane mode in Table 2.2.

2.5 Conclusion

We presented a detailed study of structure, energetics and mechanical properties of SWNTs of varying size and chirality. The determined structure and lattice parameters for closed packed (10, 10) like nanotubes are in close agreement with observations. We also determined all vibrational modes and frequencies of bulk and isolated nanotubes using a highly accurate classical force field.

2.6 References

1. Iijima, S., *Nature* **354**, 1991, 56-58.

2. Iijima, S. and Ichlhashi, T., *ibid* 1993, 603.

3. Bethune, D.S., Kiang, C.H., Devries, M.S., Gorman, G., Savoy, R., Vazquez, J., Beyers, R., *Nature* **363**, 1993, 605-607.

4. Thess, A., Lee, R., Nikolaev, P., Dai, H., Petit, P., Robert, J., Xu, C., Lee, Y.H., Kim, S.G., Rinzler, A.G., Colbert, D. T., Scuseria, G.E., Tomanek, D., Fisher, J.E., and Smalley, R.E., *Science* **273**, 1996, 483-487.

5. Krotov, Y.A., Lee D.-H., and Louie, S.G., *Physical Review Letters* **78(22)**, 1997, 4245-4248.

6. Tuzun, R.E., Noid, D.W., Sumpter,B.G., and Merkle, R.C., *Nanotechnology* **7(3)**, 1996, 241-246.

7. Ihara, S. and Itoh, S., *Surf. Rev. Lett.* **3(1)**, 1996, 827-834.

8. Cohen, M.L., *Mat. Sci. Eng. A* **209(1-2)**, 1996, 1-4.

9. Menon, M., Richter, E., and Subbaswamy, K.R., *J. Chem. Phys.* **104(15)**, 1996, 5875-5882.

10. Hamada, N., Sawada, S. and Oshiyama, A., *Phys. Rev. Lett.* **78(10)**, 1992, 1579-1581.

11. Saito, R., Fujita, M., Dresselhaus, G. and Dresselhaus, M.S., *Appl. Phys. Lett.* **60**, 1992, 2204-2206.

12. Blase, X., Benedict, L.X., Shirley, E.L., and Louie, S.G., *Phys. Rev. Lett.* **72(12)**, 1994, 1878-1881.

13. Guo, Y.J., Ph.D. Dissertation, California Institute of Technology, 1992

14. Guo, Y.J., Karasawa, N., and Goddard III, W.A., *Nature* **351**, 1991, 464-467.

15. Gao, G., Cagin, T. and Goddard III, W.A., "Where the K are in Doped Single Walled Carbon Nanotube Crystals," (on press).

16. Lim, K.T., Brunett, S., Iotov, M., McClurg, R.B., Vaidehi, N., Dasgupta, S., Taylor, S. and Goddard III, W.A., *J. Comp. Chem.* **18**, 1997, 501.

17. Landau, L.D. and Lifshitz, E.M., *Elasticity Theory, Pergamon*, Oxford, 1986.

18. Rao, A.M., Richter, E., Bandow, S., Chase, B., Eklund, P.C., Williams, K.A., Fang, S., Subbaswamy, K.R., Menon, M., Thess, A., Smalley, R.E., Dresselhaus, G., and Dresselhaus, M.S., *Science* **275**, 1997, 187-191.

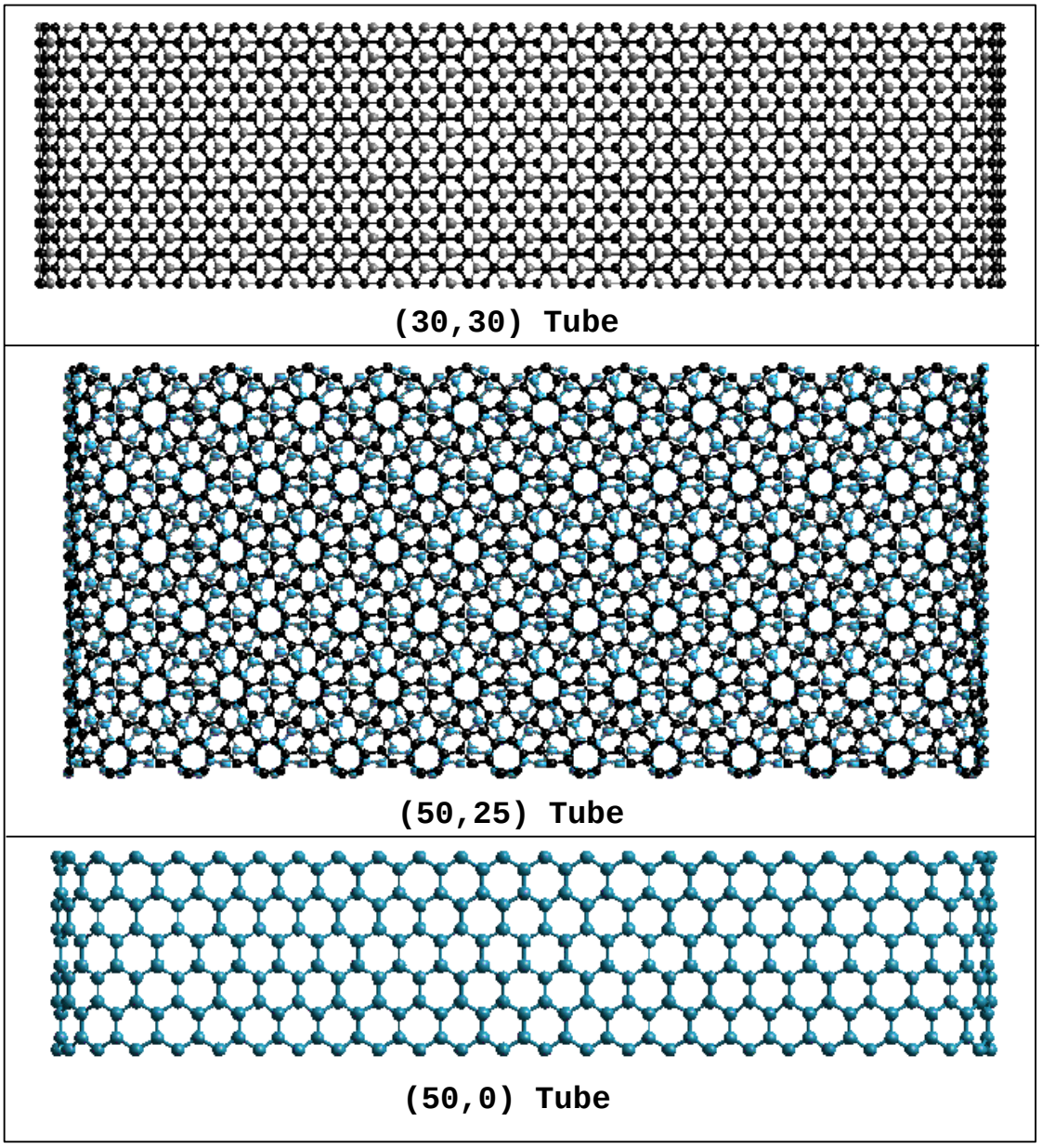

Figure 2.5: Side views of collapsed structures

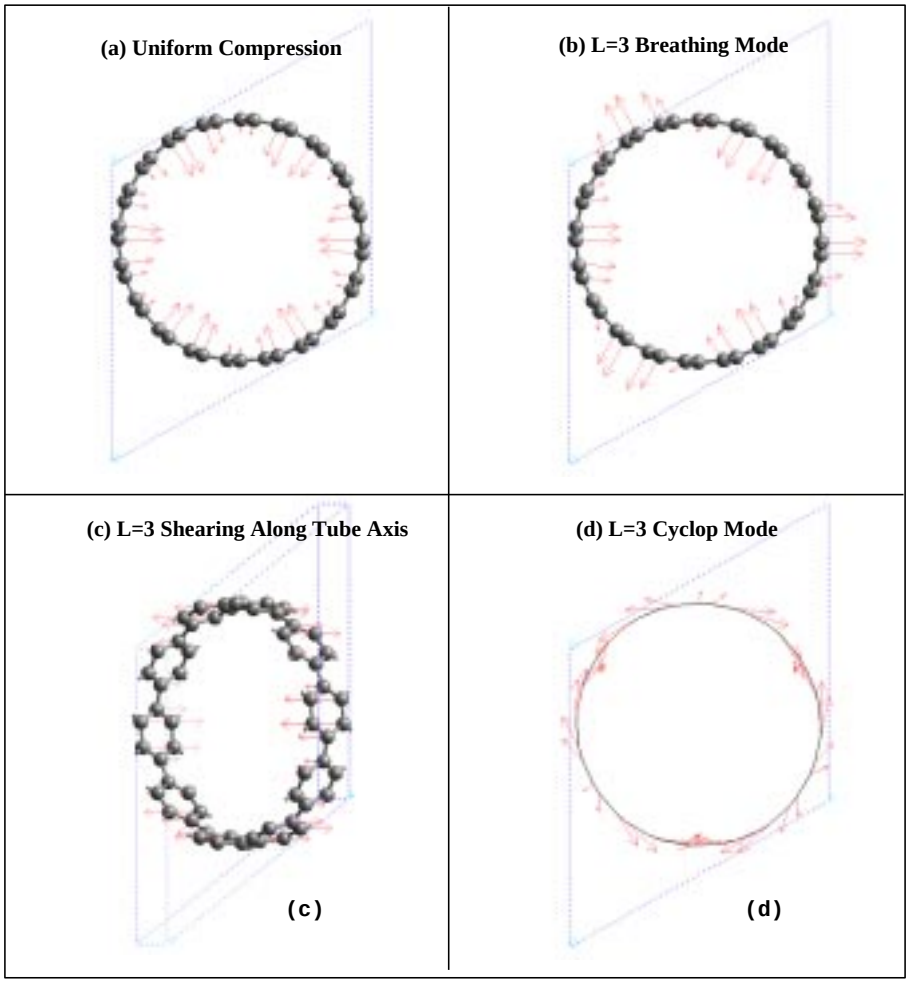

Figure 2.6: Selected vibrational modes

2.7 Tables

Table 2.1: Vibrational Modes of (10, 10), (12, 6), and (17, 0)

L	$B_{(10,10)}$	$S_{(10,10)}$	$C_{(10,10)}$	$B_{(12,6)}$	$S_{(12,6)}$	$C_{(12,6)}$	$B_{(17,0)}$	$S_{(17,0)}$	$C_{(17,0)}$
1		111	242		122	265		113	247
		112	244		122	265		113	247
2	53	223	381	59	243	412	54	227	386
	53	223	381	59	243	412	54	227	386
3	49	333	524	57	364	566	50	341	530
	55	333	530	63	364	571	57	342	535
4	127	442	671	137	483	720	128	456	675
	127	442	671	137	483	720	129	456	676
5	147	549	805	168	600	850	149	570	806
	147	549	805	168	600	850	150	570	806
6	201	652	924	229	713	976	203	683	921
	226	652	925	249	713	977	227	683	921
7	262	750		299	819	1072	267	794	1017
	272	750		299	819	1072	267	794	1017
8	328	838		360	912	1136	327	901	1091
	330	838		360	912	1136	328	901	1091
9	375	909		396			379	1002	1140
	381	909		400			385	1002	1140
10	402	939		394			434		

- Frequency in CM^{-1}.

Table 2.2: Compressing Mode and the Highest Mode

	(7, 7)	(8, 8)	(9, 9)	(12, 6)	(17, 0)	(10, 10)	(11, 11)	(12, 12)
Uniform Comp.	261	231	207	202	188	186	168	152
Highest Mode	1583	1584	1584	1585	1586	1584	1584	1584

- Frequency in CM^{-1}.

Table 2.3: Energy of Collapsed and Circular (n, n) Tubes (relative to graphite)

(n, n)	Atoms	R (Å)	$E_{circular}$	$E_{collapsed}$	(n, n)	Atoms	R (Å)	$E_{circular}$	$E_{collapsed}$
10	40	6.73	2.5418		50	200	33.66	1.3793	1.3251
11	44	7.41	2.3366		60	240	40.39	1.3641	1.2353
12	48	8.08	2.1790		70	280	47.13	1.3550	1.1715
13	52	8.75	2.0556		80	320	53.86	1.3490	1.1232
14	56	9.43	1.9571		90	360	60.59	1.3450	1.0858
15	60	10.10	1.8773		100	400	67.32	1.3420	1.0559
16	64	10.77	1.8117		110	440	74.05	1.3399	1.0313
17	68	11.44	1.7572	2.4340	120	480	80.79	1.3383	1.0109
18	72	12.12	1.7115	2.3293	130	520	87.52	1.3372	0.9939
19	76	12.79	1.6726	2.2369	140	560	94.25	1.3361	0.9791
20	80	13.46	1.6394	2.1553	150	600	100.98	1.3354	0.9659
30	120	20.20	1.4678	1.6847	160	640	107.72	1.3348	0.9552
40	160	26.93	1.4074	1.4600	170	680	114.45	1.3341	0.9452
41	164	27.60	1.4036	1.4435	180	720	121.18	1.3337	0.9362
42	168	28.28	1.4002	1.4278	190	760	127.91	1.3332	0.9284
43	172	28.95	1.3969	1.4128	200	800	134.65	1.3326	0.9211
44	176	29.62	1.3939	1.3987	210	840	141.38	1.3324	0.9146
45	180	30.30	1.3910	1.3849	220	880	148.11	1.3321	0.9088
46	184	30.97	1.3884	1.3720	230	920	154.84	1.3318	0.9035
47	188	31.64	1.3859	1.3594	240	960	161.57	1.3318	0.8984
48	192	32.31	1.3836	1.3476	250	1000	168.31	1.3317	0.8943
49	196	32.99	1.3814	1.3361	∞	∞	∞	1.3050	0.7336

- Energy in $kcal/mol$.

Table 2.4: Energy (kcal/mol) of Collapsed and Circular (n, 0) Tubes

(n, 0)	Atoms	R (Å)	$E_{circular}$	$E_{collapsed}$	(n, 0)	Atoms	R (Å)	$E_{circular}$	$E_{collapsed}$
10	40	3.89	4.7507		77	308	29.93	1.3926	1.3968
20	80	7.77	2.2446		78	312	30.32	1.3910	1.3898
21	84	8.16	2.1614		79	316	30.71	1.3894	1.3816
22	88	8.55	2.0890		80	320	31.09	1.3879	1.3743
23	92	8.94	2.0255		90	360	34.98	1.3757	1.3098
24	96	9.33	1.9697		100	400	38.87	1.3669	1.2586
25	100	9.72	1.9203		110	440	42.76	1.3604	1.2163
26	104	10.11	1.8763		120	480	46.64	1.3555	1.1818
27	108	10.49	1.8371		130	520	50.53	1.3516	1.1517
28	112	10.88	1.8019	2.5316	140	560	54.42	1.3486	1.1262
29	116	11.27	1.7702	2.4623	150	600	58.30	1.3461	1.1042
30	120	11.66	1.7416	2.3980	160	640	62.19	1.3441	1.0850
40	160	15.55	1.5623	1.9563	170	680	66.08	1.3424	1.0683
50	200	19.43	1.4788	1.7217	180	720	69.96	1.3410	1.0532
60	240	23.32	1.4333	1.5672	190	760	73.85	1.3398	1.0392
70	280	27.21	1.4058	1.4567	200	800	77.74	1.3388	1.0270
71	284	27.60	1.4037	1.4476	210	840	81.62	1.3380	1.0160
72	288	27.99	1.4016	1.4384	220	880	85.51	1.3372	1.0062
73	292	28.37	1.3997	1.4298	230	920	89.40	1.3366	0.9971
74	296	28.76	1.3978	1.4213	240	960	93.28	1.3360	0.9884
75	300	29.15	1.3960	1.4129	250	1000	97.17	1.3355	0.9808
76	304	29.54	1.3942	1.4047	∞	∞	∞	1.3050	0.7439

Table 2.5: Energy (kcal/mol) of Collapsed and Circular (2n, n) Tubes

(2n, n)	Atoms	R (Å)	$E_{circular}$	$E_{collapsed}$	(2n, n)	Atoms	R (Å)	$E_{circular}$	$E_{collapsed}$
5	140	5.14	3.3639		25	700	25.71	1.4149	1.4938
10	280	10.28	1.8579		26	728	26.74	1.4085	1.4664
11	308	11.31	1.7672	2.4559	27	756	27.77	1.4028	1.4415
12	336	12.34	1.6979	2.2969	28	784	28.79	1.3976	1.4182
13	364	13.37	1.6438	2.1660	29	812	29.82	1.3930	1.3961
14	392	14.40	1.6008	2.0572	30	840	30.85	1.3888	1.3757
15	420	15.43	1.5660	1.9660	35	980	35.99	1.3731	1.2917
20	560	20.57	1.4629	1.6690					